EFDA–JET–CP(08)01/11

M. Brix, N.C. Hawkes, A. Boboc, V. Drozdov, and S.E. Sharapov
and JET EFDA contributors

Accuracy of EFIT Equilibrium Reconstruction with Internal Diagnostic Information at JET

Accuracy of EFIT Equilibrium Reconstruction with Internal Diagnostic Information at JET

M. Brix, N.C. Hawkes, A. Boboc, V. Drozdov, and S.E. Sharapov
and JET EFDA contributors*

JET-EFDA, Culham Science Centre, OX14 3DB, Abingdon, UK

[3]EURATOM-UKAEA Fusion Association, Culham Science Centre, OX14 3DB, Abingdon, OXON, UK
** See annex of M.L. Watkins et al, "Overview of JET Results ",*
(Proc. 21 st IAEA Fusion Energy Conference, Chengdu, China (2006)).

Preprint of Paper to be submitted for publication in Proceedings of the
HTPD High Temperature Plasma Diagnostic 2008, Albuquerque, New Mexico.
(11th May 2008 - 15th May 2008)

ABSTRACT.
In tokamak experiments, equilibrium reconstruction codes are used to calculate the location of the last closed flux surface, to map diagnostic information and to derive important properties like current density and safety factor. At JET, the equilibrium code EFIT is automatically executed after each discharge. For speed and robustness intershot EFIT is based on magnetic probe measurements only. As a consequence, the intershot profiles of the safety factor can be wrong for a variety of plasma scenarios.

Internal diagnostic information, the pitch angle as measured with the Motional Stark effect, Faraday rotation angles as well as pressure profile information can increase the accuracy of the EFIT equilibrium. In this paper, the accuracy of the internal diagnostics at JET and their impact on the EFIT results are discussed in detail. The influence of control parameters like the form of the test functions for ff′ and p′ on the equilibrium is investigated. The qmin from this analysis agrees with information from MHD analysis (e.g. Alfvén cascades and sawtooth analysis) to within 10-15%.

1. INTRODUCTION INTO EFIT

EFIT is the standard equilibrium code at JET. The original EFIT by Lao [1] was adapted to incorporate the iron core of JET and the JET specific diagnostics [2, 3]. EFIT solves the Grad-Shafranov equation by adjusting the flux fit functions p′ and ff′.

$$\Delta^*\Psi = -\mu_0 R j_\phi = -\mu_0 R^2 p'(\Psi) - \mu_0{}^2 f(\Psi) f'(\Psi) \qquad (1)$$

The accuracy of the results depends on the quality and availability of the diagnostic information and on the EFIT settings like the functional representation of p′ and ff′. An automatic version of EFIT is executed after each pulse to deliver information on the basic plasma geometry for diagnostic mapping. For speed and robustness intershot EFIT is based on magnetic probe measurements only. The equilibrium problem is ill posed without internal diagnostic information; as a consequence, the inter-shot profiles of the safety factor and current density can be inaccurate in particular plasma scenarios. An example is presented in section 3 (see figs 4 and 6).

2. INTERNAL DIAGNOSTICS AT JET

A. MOTIONAL STARK EFFECT DIAGNOSTIC

The Motional Stark Effect diagnostic (MSE) delivers spatially resolvedmeasurement of the projected magnetic pitch angle γ_m close to the equatorial plane. By its very nature it requires neutral beam injection. The fast neutral beam deuterium atoms (E = 125-130kV) experience the magnetic field as an electric field $E_L = \mathbf{v} \times \mathbf{B}$, the resulting Stark split radiation is polarised with respect to E_L. If the beam is observed at a non perpendicular direction, the resulting Doppler shift allows the emission of the MSE beam to be distinguished from background H and beams. More details on the MSE implementation at JET can be found in [4].

Under ideal measurement conditions at low to inter-mediate heating power, the MSE at JET allows a temporal resolution of t=10ms, 20–40ms is more typical. The radial resolution is of the order of 5-8cm. However, in discharges with high levels of additional heating, the MSE measurement can be significantly distorted by strong ELM activity, by hot spots on the LH launcher, the RF antenna or the poloidal limiters (see fig.1) and the edge channels can be distorted by increased levels of CII radiation at $\lambda = 658$nm . Under such conditions, the quality of the MSE data can often be improved by modulation of the MSE beam, which allows discrimination of MSE beam emission and polarized background radiation. This reduces the effective temporal resolution of MSE constrained EFIT equilibria to the modulation frequency, typically 2-10Hz.

The MSE data have to be validated before using them in the equilibrium code. Some channels have to be deselected for time slices where the measurement is too distorted. This is usually done manually by checking the smoothness of radial profiles of the pitch angle γ_m. Furthermore, the plasma radial electric field is calculated from the toroidal rotation (from charge exchange recombination spectroscopy [5]) and the poloidal field (from MSE B_z) and subtracted from the measured electric field to obtain the Lorenz field only. More details on beam modulation and MSE calibration can be found in [6].

B. FARADAY ROTATION

The setup for the interferometer-polarimeter allows a measurement of the line integrated density and Faraday rotation along the same lines of sight. A successful analysis of the line integrated Faraday rotation $\alpha = \int n_e \mathbf{B} \cdot d\mathbf{l}$ requires an accurately known density profile. EFIT calculates a density profile from the line integrated interferometer measurement by fitting the density profile with low order polynomials. In the current EFIT version only low order polynomials have proven to be numerically stable; this has consequences on the type of density profiles which can be reconstructed. For the interpretation of the Faraday rotation measurement, it proved to be useful to use only channels 3 and 5-8 from the interferometer (fig.2). Channel 1 lies usually outside the plasma, the density measurement with channels 2 and 4 is not robust (small feedthroughs in the divertor, beam refraction effects). Furthermore, channel 4 is often close to or in the steep gradient region at the plasma edge (e.g. in H-mode plasmas, see fig.3). Complex density profiles cannot be fitted with the existing basis functions. A completely rewritten version of EFIT is under development. This code is intended to use density profile information from a high resolution Thomson scattering diagnostic and should increase the accuracy of the interpretation of the Faraday rotation effect.

C. PRESSURE PROFILE

There are various ways of calculating a pressure profile depending on the availability of diagnostic data.

- The simplest approach is to assume electron and ion pressure to be the same, $p_e = p_i$, and to use p_e from LIDAR (the JET Thomson scattering diagnostic [8]). This is only done when no

charge exchange ion temperatures T_i are available.

- After each pulse a sequence of automatic analysis codes CHAIN1 [9] is executed. The Fokker-Planck beam deposition code PENCIL [10] calculates the perpendicular and parallel energy densities of the neutral beam born fast particles $W_\perp$ and $W_{||}$. If the charge exchange T_i is available, a pressure profile can be constructed from the thermal p_i and p_e and from the fast particle pressures $p_\perp$ and $p_{||}$, which are calculated from the fast particle energy densities $W_\perp$ and $W_{||}$.
- A second sequence of analysis codes CHAIN2 [11] is available upon request after data validation. CHAIN2 provides fast particle energy densities for ion cyclotron resonance heating (PION [12]) and neutral beam heating PENCIL and pi based on Z_{eff}, n_i and T_i from charge exchange impurity analysis.

A correct treatment of anisotropic pressures requires a modified Grad-Shafranov equation [18]. In this paper, like in TRANSP [13], we use the scalar sum of the pressure components in the unmodified Grad-Shafranov equation [14]:

$$p_{MHD} = p_e + p_i + \frac{p_\perp + p_{||}}{2} \qquad (2)$$

The pressure information is usually based on the magnetics only intershot EFIT mapping. To avoid inconsistencies in particular in the plasma centre, the pressure is only constrained for major radii $3.3m < R < 3.8m$.

3. EXAMPLES FOR EFIT ANALYSIS AND CROSS CHECK WITH MHD INFORMATION

The following examples show, for different plasma scenarios, results of differently constrained EFIT runs. Fig.4 shows the temporal evolution of q_{min} for a sawtoothing plasma. Intershot, magnetics only EFIT fails to correctly predict the minimum value of the safety factor q_{min}. The qmin from a combined MSE, pressure, Faraday rotation and magnetics constrained EFIT run (EFTM) is shown for comparison. The radius of the EFTM q_{min} =1 surface is about 10cm larger than the sawtooth inversion radius derived from soft-X analysis (similar results are reported in [15]).

Only the MSE diagnostic has the spatial resolution to detect current holes in the plasma centre [16]. It is not straight forward to analyse current holes with EFIT even if flexible splines or high order polynomials are used (in this paper 6-knot splines are used to represent ff', for the current hole pulses additional spline knots are used at $\Psi \leq 0.1$). Therefore in the past, a two step, so called fixed-Ψ analysis method has been used to determine the current hole equilibrium (for details see [17]).

Recently, we found that current holes can be fitted by using the EFIT constraint RELAX. RELAX slows down the convergence by increasing the impact of older iteration steps. The benefit of the

RELAX method is that a proper solution of the Grad-Shafranov equation is found at the expense of increased computation time and reduced accuracy of the MSE fit at the edge of the current hole. In figs.5 and 6 the q-profile and qmin from EFTM equilibria are compared with MHD data. In both cases excellent agreement with qmin from Alfv´en [19] and sawtooth analysis is found.

The qmin from EFTM has been compared with MHD data for about 40 pulses at different discharge conditions. Provided that the MSE data is of reasonable quality, the data agrees within typically 10–15% .

4. IMPACT OF FARADAY ROTATION DATA ON COMBINED ANALYSIS

Whereas the MSE measurement is located close to the equatorial plane, the line integrated Faraday rotation contributes with measurements above and below the mid- plane. Whilst maintaining a similar fitting accuracy of the MSE data, incorporating the Faraday rotationmainly changes the plasma elongation (check the difference between the solid and dashed flux surfaces in fig.2). In shear reversed plasmas, utilizing the Faraday rotation data as an additional constraint results in an increase of qmin by 10%. Fig.7 illustrates the effect, the shear is reversed prior to $t \approx 6.8$s and monotonic for later times.

SUMMARY AND CONCLUSIONS

The accuracy of the EFIT equilibrium can be significantly increased by incorporating internal diagnostic information. Combining the high spatial resolution of the Motional Stark effect diagnostic with the line integrated Faraday rotation measurements and constraining a reasonable pressure profile results in profiles of the safety factor which agree with qmin and inversion radii from sawtooth analysis and qmin from Alfvén cascades within 10–15%. The accuracy of the Motional Stark Effect diagnostic at JET can be increased by modulation of the MSE diagnostic beam. Future work should benefit from incorporating Thomson scattering density profiles for the analysis of the Faraday rotation.

ACKNOWLEDGMENTS

This work has been carried out under the European Fusion Development Agreement, supported by the European Community. The views and opinions expressed herein do not necessarily reflect those of the European Commission.

REFERENCES

[1]. L.L. Lao et al., Nuclear Fusion **25** (1985) 1421
[2]. D.P. O'Brien et al., Nuclear Fusion' **32** (1992) 1351
[3]. W. Zwingmann et al., proc. 7th European Fusion Theory Conference, Jülich (1997)
[4]. B.C.Stratton et al., Rev. Sci. Instrum. **70** (1999) 898
[5]. C.R. Negus et al., Rev. Sci. Instrum. **77** (2006) 10F102 and C. Giroud et al, this conference

[6]. N.C. Hawkes, M. Brix, Rev. Sci. Instrum. **77** (2006) 10E509
[7]. G. Braithwaite et al., Rev. Sci. Instrum. **60** 2825 (1989)
[8]. C. Gowers et al., J. Plasma Fusion Research **76** (2000) 874-877
[9]. J.P. Christiansen, Comp. Physics **73** (1987)85
[10]. C.C. Challis et al., Nucl. Fusion **29** (1989) 563
[11]. S.A. Arshad, Fusion Sci. Tech. **53** (2008)667
[12]. L.-G. Eriksson et al., Nucl. Fusion, **33** (1993)1037
[13]. R.J. Goldston et al., J. Comput. Phys. **43** (1981) 61
[14]. W.A. Cooper, A. J. Wootton Plasma Physics **24** (1982) 1183
[15]. H Solwitsch, H. R. Koslowski, Plasma Phys. Control. Fusion **37** (1995) 667-678
[16]. N.C. Hawkes et al., Phys. Rev. Letters **87** (2001) 115001-1
[17]. N.C. Hawkes et al., Plasma Phys. Control. Fusion **44** (2002) 1105-1125
[18]. W. Zwingmann et al., Plasma Phys. Control. Fusion **43** (2001) 1441-1456
[19]. S.E. Sharapov et al., Physics of Plasmas **9** (2002) 2027- 2036.

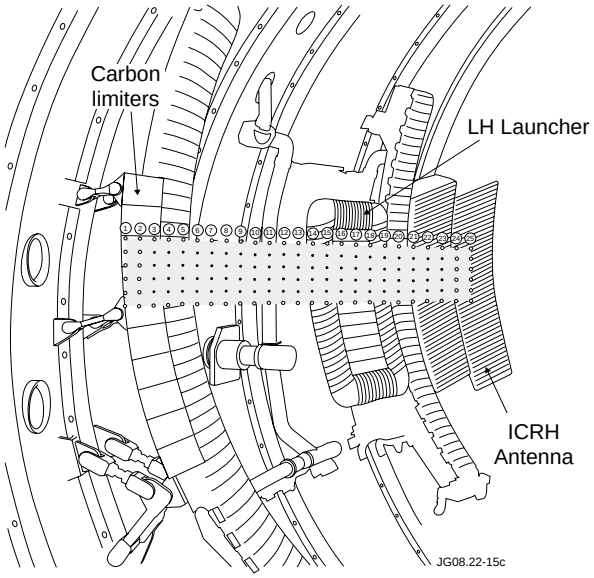

Figure 1: Projection of the MSE lines of sight on the wall.

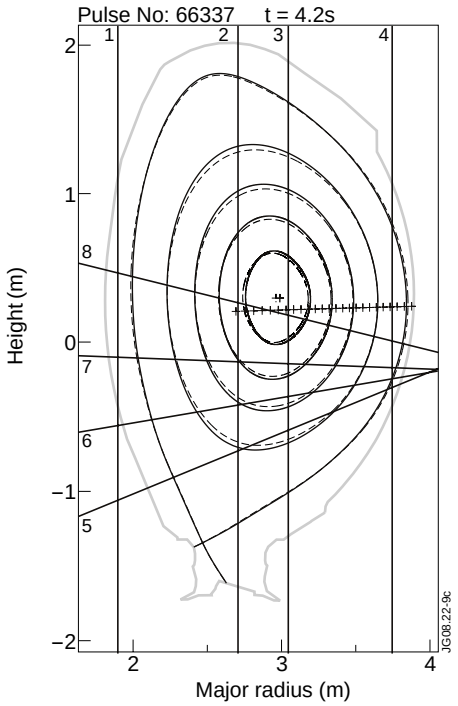

Figure 2: Lines of sight of the Faraday rotation measurement (1-8) and the location of the MSE measurement (+). The solid and dashed flux surfaces show EFIT results including and excluding the Faraday rotation diagnostic (see section IV).

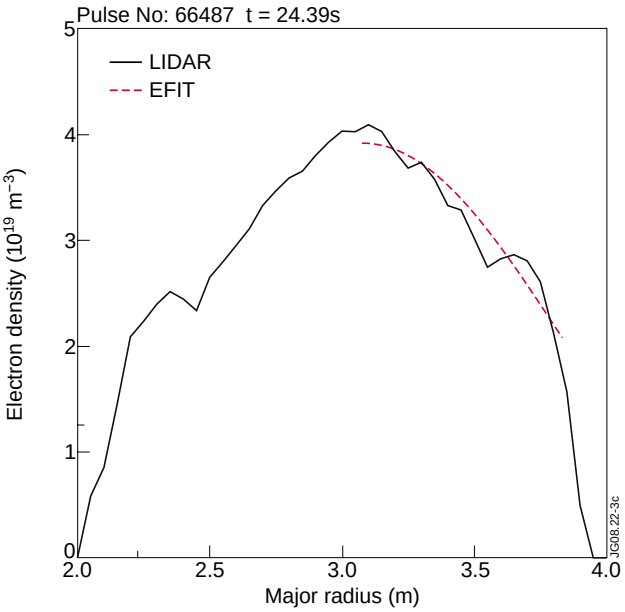

Figure 3: Comparison of LIDAR (Thomson scattering) density profile with the density profile calculated by EFIT from the line integrated interferometer.

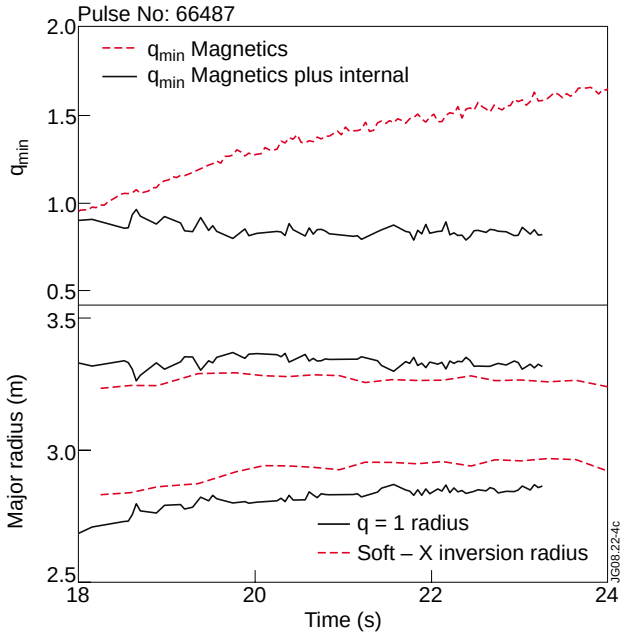

Figure 4: top: comparison of qmin from magnetics only EFIT (dashed) with q_{min} from EFTM (solid)bottom: comparison of sawtooth inversion radii from soft-Xray analysis (dashed) with q=1 surface from EFTM (solid)

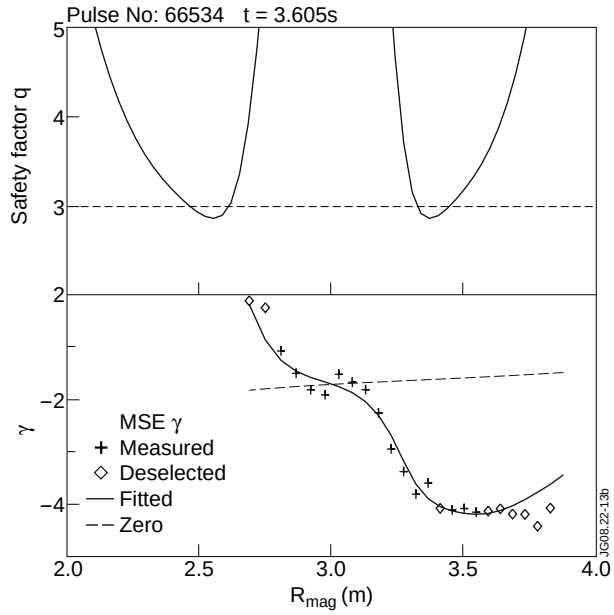

Figure 5: A current hole plasma at B_t = 3.2T : (top) q-profile for combined EFTM analysis; (bottom) measured and fitted MSE data. The observation of an Alfvén grand cascade indicates integer q_{min} at t=3.75s, which is in excellent agreement with the q_{min} =2.9 from the EFTM equilibrium.

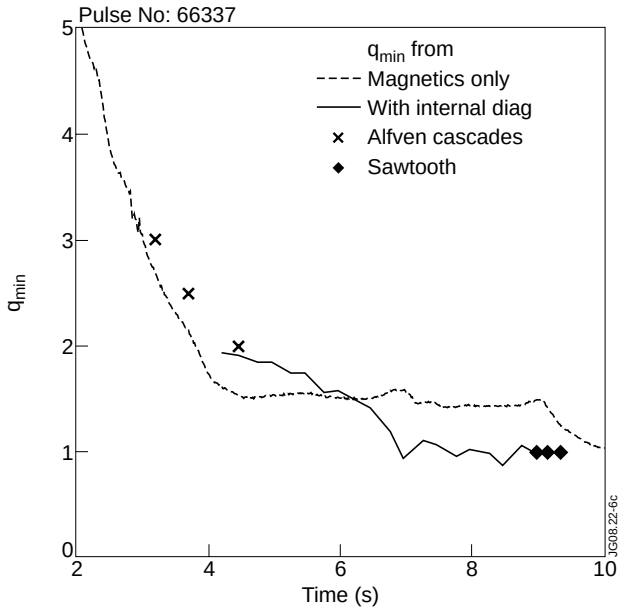

Figure 6: Comparison of q_{min} from differently constrained EFIT runs with qmin from MHD analysis for a shear reversed plasma with B_t = 2.9T.

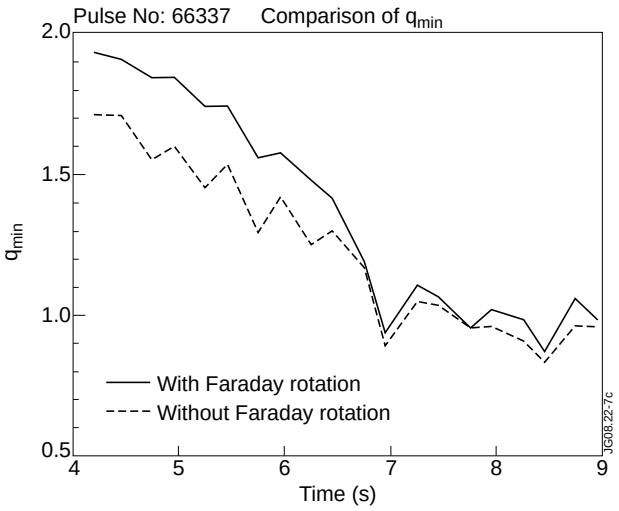

Figure 7: Impact of the Faraday rotation on the q_{min} of the combined analysis.